# Predicting the bactericidal efficacy of solar disinfection (SODIS): from kinetic modeling of in vitro tests towards the in silico forecast of E. coli inactivation

AUTHOR(S)

Sofia Samoili, Giulio Farinelli, José Á Moreno-SanSegundo, Kevin McGuigan, Javier Marugán, César Pulgarín, Stefanos Giannakis

CITATION

Samoili, Sofia; Farinelli, Giulio; Moreno-SanSegundo, José Á; McGuigan, Kevin; Marugán, Javier; Pulgarín, César; et al. (2021): Predicting the bactericidal efficacy of solar disinfection (SODIS): from kinetic modeling of in vitro tests towards the in silico forecast of E. coli inactivation. Royal College of Surgeons in Ireland. Journal contribution. https://hdl.handle.net/10779/rcsi.17307134.v1

HANDLE

10779/rcsi.17307134.v1

Chemical Engineering Journal 427 (2022) 130866

Contents lists available at ScienceDirect

Chemical Engineering Journal

journal homepage: www.elsevier.com/locate/cej

# Predicting the bactericidal efficacy of solar disinfection (SODIS): from kinetic modeling of *in vitro* tests towards the *in silico* forecast of *E. coli* inactivation

Sofia Samoili [a,1], Giulio Farinelli [b,c], José Ángel Moreno-SanSegundo [d], Kevin G. McGuigan [e], Javier Marugán [d], César Pulgarín [b,f], Stefanos Giannakis [g,*]

[a] European Commission, Joint Research Centre (JRC), Seville 41092, Spain
[b] School of Basic Sciences (SB), Institute of Chemical Science and Engineering (ISIC), Group of Advanced Oxidation Processes (GPAO), École Polytechnique Fédérale de Lausanne (EPFL), Station 6, CH-1015 Lausanne, Switzerland
[c] Department of Environment, Land and Infrastructure Engineering (DIATI), Politecnico di Torino, Corso Duca degli Abruzzi 24, 10129 Turin, Italy
[d] Department of Chemical and Environmental Technology, ESCET, Universidad Rey Juan Carlos, C/Tulipán s/n, 28933 Móstoles, Madrid, Spain
[e] Department of Physiology & Medical Physics, RCSI University of Medicine and Healthcare, Dublin D02 YN77, Ireland
[f] Colombian Academy of Exact, Physical and Natural Sciences, Carrera 28 A No. 39A-63, Bogotá, Colombia
[g] Universidad Politécnica de Madrid (UPM), E.T.S. Ingenieros de Caminos, Canales y Puertos, Departamento de Ingeniería Civil: Hidráulica, Energía y Medio Ambiente, Unidad Docente Ingeniería Sanitaria, c/ Profesor Aranguren, s/n, Madrid ES-28040, Spain

ARTICLE INFO

*Keywords:*
Solar disinfection (SODIS)
E. coli inactivation
Static model
Dynamic simulation
Water treatment

ABSTRACT

In this study, the possibility of predicting the efficacy of Solar water disinfection (SODIS) for the removal of bacterial pathogens was assessed by the development of a three-level plan: firstly, systematic *E. coli* inactivation was performed (*in vitro*) in Lake Geneva water, under otherwise controlled conditions of water temperature (20–50 °C), sunlight intensity (0–1200 W/m$^2$), presence of natural dissolved organic matter (DOM, 0–6 mg/L) and turbidity (0–50 NTU). As a second step a kinetic evaluation led to the selection of the most relevant parameters to be included in a novel static and dynamic model theoretical formulation. The static and dynamic models reliably described the experimental findings (bacterial inactivation under various climatic conditions) and were considered as equally eligible candidates for disinfection modeling. The final step considered ambient temperature, incident radiation and cloud-cover data to forecast (*in silico*) SODIS efficacy in Africa as a case study. The simulation results were compared with the experimental data and indicated that most African regions are suitable for SODIS processes, but there are areas of risk correlated with climatological conditions (cloud-cover and temperature). The results of this study could be applied for regional in decision-making strategies for application of SODIS or in the search for viable alternatives to SODIS in cases where it is deemed unsuitable.

## 1. Introduction

Solar water disinfection (SODIS) is a World Health Organization (WHO)-accepted process for the treatment of biologically contaminated water, specifically targeting waterborne pathogens and their inactivation before its consumption [1]. By definition, it uses the action of sunlight in a process that has been intuitively known for many years but only systematically practiced over the last 30 years [2]. This method has been proposed as a solution in emergency situations or as a permanent, viable alternative to chlorination, filtration or boiling, for resource-poor settings in low-to-middle-income-countries (LMICs), especially in isolated regions. The abundantly available sunlight in the majority of

*Abbreviations:* DHI, Diffuse Horizontal Irradiation; DNI, Direct Normal Irradiation; DOM, Dissolved Organic Matter; GHI, Global Horizontal Irradiation; IR, Infrared; NOM, Natural Organic Matter; PET, Polyethylene terephthalate; RSE, Residual Standard Error; SODIS, Solar Disinfection; TIR, Total Incident Radiation; TOC, Total Organic Carbon; UV, Ultraviolet; VIF, Variance Inflation Factor; WHO, World Health Organization.

* Corresponding author.
*E-mail address:* stefanos.giannakis@upm.es (S. Giannakis).

[1] Disclaimer: The views expressed are purely those of the author and may not in any circumstances be regarded as stating an official position of the European Commission.

https://doi.org/10.1016/j.cej.2021.130866
Received 21 February 2021; Received in revised form 28 May 2021; Accepted 12 June 2021
Available online 19 June 2021

LMICs can provide sufficient disinfecting potential, despite the possible complications that changeable weather conditions might cause [3].

The practice of SODIS is simple and consists solely of filling a transparent container with available water and exposing it to direct sunlight for 1 day. However, the mechanisms that govern the process are more complicated than first appear and are a matter of intense investigation. In brief, UVA has well documented efficiency in the inactivation of key components of cells [4,5] and result in the production of an excess of oxidative species, such as $H_2O_2$ [6] and Fe [7]. An intracellular photo-Fenton process can be also be initiated which is fatal to the cell [8,9]. Recently, the inactivation of key enzymes was observed as a critical component in SODIS [10] and the long-proposed synergy between heat and light [11] was quantified [12] and verified in field tests in a series of reactors [13]. Nevertheless, other more parameters must affect the global outcome of the process, which can be accounted for by the observed residual error in the aforementioned models. Dissolved organic matter (DOM) or ionic composition have been proposed as possible candidates [14–16]. In addition to the irradiance and temperature of the water [11,17–21], a systematic study of key parameters is necessary to complement the current literature.

The complexity of the pathways leading to disinfection have initiated a separate sub-field of investigations dedicated to modeling the inactivation process, as a means of describing and predicting the outcome of solar exposure on the degree of inactivation achieved. The most common approach deals with the characterization of disinfection curves, adapting mathematical expressions from adjacent disinfection fields, such as food sterilization by heat or UV [22]. The model expressions usually applied are the (modified) Chick-Watson, the Hom or similar type of empirical model [23], while the log-linear model with a delay period [24] has been proven to provide a good fit in a series of works [25–28]. Furthermore, similarly to other disinfection applications, SODIS demands a certain level of prediction of the success of the potential application, hence the early approaches of "single-hit, multi-target" or "multi-hit, single-target approaches [29] have evolved into stochastic models attempting to describe bacterial disinfection [30]. Nevertheless, the problem with empirical models is that they cannot offer significant insight into the disinfection process, as they tend to describe in mathematical terms the natural phenomenon with little natural significance or are over-fitted to describe a process, without a prediction capacity beyond the experimental space. In this sense, new models are called for, that have prediction potentials and incorporate the basic physicochemical and biological aspects of solar-thermal disinfection.

In this study, we have implemented a multi-level, poly-parametric study of surface water disinfection (the Swiss Lake Geneva), by means of solar radiation, as a basis to harvest the necessary data and propose a new model that will predict the inactivation efficiency for SODIS in other candidate countries. More specifically, sunlight intensity, water temperature, Dissolved Organic Matter (DOM) content and turbidity, were chosen as independent variables, and the bacterial inactivation as the response. We aim to estimate and predict the bacterial inactivation by discretization of the possible environmental conditions, in order to develop a novel dynamic (time-resolved) model. Finally, an attempt to forecast the SODIS efficacy across the African continent was made as a case study: using ambient temperature and incident radiation values collected from open-source databases, and by applying the data acquired in the laboratory tests, the geographical distribution of the inactivation efficiency in the African continent was predicted *in silico*.

## 2. Materials and methods

### 2.1. Chemicals and reagents

For the simulation of higher quantities of organic matter in water, Suwannee river NOM (reverse osmosis isolate, 2R101N) was purchased from the International Humic Substances Society (IHSS). Similarly, for the addition of suspended solids to simulate higher turbidity, kaolin (china clay) was used as received, purchased from Sigma-Aldrich. NaCl, KCl, Plate count agar and Select Yeast Extract used for the preparation of sterile bacterial growth and dilution media were also purchased from Sigma-Aldrich. BactoTryptone™ was purchased from BD and the water used for the preparation of the saline solutions, growth media and agar was Mili-Q, from a Milipore (Merck) Elix apparatus (~15.8 MΩ.cm).

### 2.2. Experimental details

#### 2.2.1. Light source and reactors

Light was provided through a bench-scale CPS Suntest solar simulator (Atlas). The simulator is equipped with a Xenon lamp and illuminates a surface area of 560 $cm^2$. The spectral composition is as follows: 0.5% UVB (290–320 nm) ~ 5% UVA (320–400 nm) and the rest (up to 800 nm) follows the solar spectrum (see supplementary Fig. S1). A UVC and an infrared (IR) cut-off filter ensure transmission in the aforementioned wavelengths, while the system is air-cooled by ventilators. Global irradiance was monitored by a pyranometer-radiometer couple (Kipp&Zonen) and set at discrete levels, namely 0 (shut down), 400, 800 and 1200 $W/m^2$. The chosen irradiance values correspond to weak, moderate, and the approximately the maximum light irradiance values reaching earth's surface.

The reactors used were 4 cylindrical, double-wall, Pyrex glass rectors, with dimensions corresponding to 9 cm height, 6.5–7.5 cm inner-outer diameter (see supplementary Fig. S2). Their peripheral walls are opaque hence it is assumed that no lateral light penetration occurs. Hence, light is introduced from a 30-$cm^2$ opening on the top. Water recirculating within the double walls of the reactors by means of a thermostat ensured effective control of water temperature (accuracy: ±0.5 °C). Furthermore, a borosilicate glass, cover was placed on top to reduce UVB transmissibility and better simulate the SODIS field-conditions for polyethylene terephthalate (PET) or glass SODIS bottles, which almost completely block UVB irradiation (see supplementary Fig. S3). A magnetic bar was placed inside the reactors to induce stirring (350 rpm), while the whole system was placed on a magnetic stirrer. After each experiment, the reactors were washed with acid to remove organic matter and water minerals, rinsed multiple times with demineralized water and finally autoclaved (121°C).

#### 2.2.2. Water matrix: Lake Geneva water characteristics

In order to better simulate the natural water matrix and induce the temporal variability factor, weekly samples of lake water were collected from Lake Geneva (coordinates: 46°30′33.3″N, 6°33′44.9″E) and used as sampled (no filtration or pre-treatment). The samples were always stored in a refrigerated environment (~4 °C). Experiments on the samples started only after they reached room temperature. The average physicochemical characteristics of the water for the duration of the sampling campaigns fall within the normal ranges for natural waters [31] and are given in detail in Table 1.

For experimental purposes, in order to achieve the levels of NOM (in TOC-mg/L units) and turbidity observed in Table 1, the water was incrementally enriched with aliquots of a concentrated NOM or kaolin solution, respectively until the target values of TOC and turbidity were achieved.

**Table 1**
The physicochemical properties of Lake Geneva water.

| Parameter | Lake Geneva water | Units |
|---|---|---|
| pH | 8.3–8.7 | |
| Total organic carbon (TOC) | 0.8–1 | (mg/L) |
| Turbidity | 0.5–0.7 | NTU |
| Hydrogen carbonate | 100–120 | (mg/L) |
| Chloride | 8–10 | (mg/L) |
| Sulfates | 48–55 | (mg/L) |
| Nitrates | 1.5–3.1 | (mg/L) |

#### 2.2.3. Experimental design

For the proper assessment of the effects and interactions of the variables involved in the SODIS process, a full-factorial experimental design was conceived and executed as described below:

The following independent variables were chosen: global irradiance (I, W/m$^2$); water temperature (T, °C); concentration of organic matter (DOM, mg/L TOC); turbidity (NTU); exposure (time t, min). Bacterial decay (inactivation, logU) was the response variable. Table 2 presents a summary of the tests, including the independent, dependent variables and the corresponding levels. The data with the bacterial inactivation results can be found online [32].

Concerning the organic matter content of the water used for SODIS, since Lake Geneva water contains relatively low quantities of DOM, 0 corresponds to "no further NOM addition" and 6 to "required addition in order to reach 6 mg/L TOC", respectively. For turbidity simulation, 0 similarly means no kaolin addition and 50 means we added the necessary amount of kaolin particles in order to reach a turbidity of 50 NTU.

### 2.3. Microbiological methods

#### 2.3.1. Bacterial strain preparation

*Escherichia coli* K-12 wild type strain was acquired from Deutsche Sammlung von Mikroorganismen und Zellkulturen, (DSMZ No. 498) and was used as a bacterial pathogen indicator proxy, as suggested by the World Health Organization [33]. The detailed procedure is published elsewhere [19]. Bacteria stored in cryo-vials were used to create the initial inoculum on agar, from which a colony was picked and cultivated in Luria-Bertani Broth (LB) for 8 h, under constant agitation at 37°C in the dark. After 8 h, 1% dilution took place in LB and the strain was grown for 15 more hours till the stationary growth phase was reached. Purification of the strain took place by centrifuging for 15 min (5000 rpm at 4°C) and washing twice with isotonic saline solution (5 min, 5000 rpm, at 4°C with NaCl/KCl). The final pellet was dispersed in saline solution reaching a stock solution of $10^9$ CFU/mL. Spiking of lake water was fixed at $10^6$ CFU/mL just before experimentation.

#### 2.3.2. Bacterial plating and enumeration

Determination of bacterial concentration was carried out following a previously published protocol [34]. Briefly, 1-mL samples were drawn from the body of the solution in the glass reactors and were immediately plated. Bacterial enumeration was by the standard plate count method, with 0.1 mL samples on 9-cm Petri dishes, containing non-selective plate count agar (PCA). Experiments were performed in duplicate (statistical replicates) on two separate occasions (biological replicates). In order to achieve countable dishes, serial dilution took place, and 2 consecutive dilutions were plated (technical replicates); the values shown in the graphs represent the mean and a standard deviation of $< 15\%$ was measured (error bars not shown for clarity of the figures).

### 2.4. Bacterial inactivation modeling by GInaFiT

In order to define the basic characteristics of the solar disinfection process, all cases were treated according to the following well-established model within disinfection studies, via the GInaFiT Microsoft Excel Add-in [22]:

Shoulder/log-linear model [22,24]:

$$N = N_0 \times e^{(-kmax \times t)} \times \left(e^{(-kmax \times Sl)}\right) / \left(1 + \left(e^{(-kmax \times Sl)} - 1\right) \times e^{(-kmax \times t)}\right) \quad (1)$$

Where:

$N$ is the number of viable bacteria at time t;
$N_0$ is the initial number of bacteria at time 0;
$k_{max}$ is the slope of the regression (min$^{-1}$);
$t$ is time (min)
$Sl$ is the lag phase (Sl: shoulder length) (min)
For identification purposes this equation can be re-arranged as:

$$Log_{10}(N) = Log_{10}(N_0) - k_{max} \times t / Ln(10) + Log_{10}\left(e^{(kmax \times Sl)}\right) / \left(1 + \left(e^{(kmax \times Sl)} - 1\right) \times e^{(-kmax \times t)}\right) \quad (2)$$

### 2.5. Statistical analyses

#### 2.5.1. Static and dynamic modeling of bacterial inactivation: Theory and models

In this section linear regression modeling is employed, in order to formulate the models describing bacterial inactivation. Linear regression is an approach to modeling which predicts the relationship of $\zeta$ number of explanatory variables $X$ to scalar response variables $Y$, with linear functions. The $X$ are also referred to as independent, explanatory, input, predictor or exogenous variables or covariates or regressors. The $Y$ are also called dependent, response, measured variables or regressands. To delineate bacterial concentration dynamics and provide an accurate insight into solar mediated bacterial inactivation in surface waters, multiple regression models are employed in the section in question. These models are linear in terms of estimation, as the regression function is linear to the coefficients $\beta$, the unknown parameters of the independent variables. Hence, by considering the independent variables of the model as distinct variables, the techniques of multiple regression are used to compute the polynomial regression for a least square analysis. Furthermore, it should be noted that in the static expression of the models, the order of the observations does not affect the estimation of the variables, and a one-regressor model is of the form $Y_i = a + \beta_i X_i + \varepsilon_i$, with $a, \beta_i$ constant coefficients $\in \mathbb{R}\backslash\{0\}$, and $\varepsilon_i$ $N(0, \sigma^2)$ representing the residual errors that follow a normal distribution. On the other hand, in the dynamic regression models, the variables evolve over time, so the observations are ordered by time. Therefore, starting from a static multivariate model $Y_i = \beta_0 + \beta_1 X_{i_1} + \cdots + \beta_r X_{i_r} + \varepsilon_i$, the dynamic expression as an autoregressive process under the assumption that the observations of the independent variables $X$ at time $t$ are related to one time step before and one after. The model can be written by including a lagged value of the dependent variable $Y$ on the right hand-side of the expression accompanied by the other explanatory variables, as such $Y_{i,t} = \varphi Y_{i,t-1} + \beta_0 + \beta_1 X_{i_1,t} + \cdots + \beta_r X_{i_r,t} + \varepsilon_{i,t}$. In this expression the process errors follow a multivariate normal distribution.

#### 2.5.2. Statistical assessment of forecasting performance

With regression, the model uses observed values for the variables to estimate predicted values of inactivation. The difference between observed and predicted values is described by the residual error term $\varepsilon_i$. Therefore, to predict the response variable, measurement of the residual error term is required. The regression models developed are assessed through the estimation of the residual error term, specifically an estimate $\widehat{\varepsilon}_i$ of the standard deviation of the sample of the given dataset. This error term allows us to measure the magnitude of difference between an observation of the sample and the sample mean, which indicates the quality of the regression fit to the given dataset. Using a least-squares regression approach, the estimated errors $\widehat{\varepsilon}_i$ are assumed to follow a normal Gaussian distribution, and are computed by the differences be-

**Table 2**
Experimental Design specifications.

| Variables | Units | Levels |
|---|---|---|
| Irradiance | W/m$^2$ | 0, 400, 800, 1200 |
| Water temperature | °C | 20, 30, 40, 50 |
| Organic Matter | mg/L | 0, 6 |
| Turbidity | NTU | 0, 50 |
| Time | min | 0–420 |
| ***Response Variable*** | | |
| Inactivation | logU (CFU/mL) | |

tween the empirical observations $Y_i$ and the predicted $\widehat{Y}_i$ (Equation (1)). The residuals' assumption of normality is confirmed by corresponding Q-Q plots.

$$\widehat{\varepsilon}_i = Y_i - \widehat{Y}_i = Y_i - (\widehat{a} + \widehat{\beta} X_i) \tag{3}$$

To render the estimated errors unbiased, the square root of variance is divided by the number of observations and variables involved. More explicitly the squared sum of the estimated errors is divided by $df = n - p - 1$, resulting in the residual standard error $\widehat{\sigma}$, where $df$ are the statistical degrees of freedom of the model, $n$ are the number of observations, and $p$ the number of independent variables involved to estimate the model (Equation (2)):

$$\widehat{\sigma} = \sqrt{\frac{\sum_{i=1}^{n} \left(\widehat{\varepsilon}_i\right)^2}{n - p - 1}} \tag{4}$$

The residual standard error is used to assess the absolute fitness of the model to the data. The lower values indicate that the model predicts the dependent variable with low standard deviation of the unexplained variance due to involved variables from the true regression line.

To evaluate the goodness-of-fit of the regression, we use the adjusted $R^2$. The $R^2adj.$ is a version of the coefficient of determination $R^2$, the latter being used to assess the relative fit between the averaged observed and predicted data. It penalizes independent variables considered in the model during its development, when they add variance without contributing to the explanation of the regression, as it uses the degree of freedom as shown in Equation (3):

$$R^2_{adj} = 1 - \left(1 - R^2\right) \frac{n - 1}{n - p - 1} \tag{5}$$

where $n$ is the number of observations with which the model is developed, $p$ is the number of independent variables, and $n - p - 1$ is the degree of freedom. Therefore, adjusted $R^2$ is inversely related to the number of independent variables that are added in the model, while being proportional to $R^2$. A value of adjusted $R^2$ close to 1 indicates that the model explains the data better than a naïve model (average of all samples) with approximately zero error. Thus, as a statistical indicator of a model it is better than $R^2$, because it has both a penalization and a rewarding factor, as well as being able to correlate the independent variables more efficiently. The regression models and the statistical analyses are developed in the R language (version 3.5) and the R Stats Package.

### 2.6. Sunlight intensity values, cloud coverage measurements and temperature databases

To estimate the disinfection rate, values of both incident radiation and temperature are required. To calculate them based on the yearly summarized values available in open databases, some assumptions were considered. As a first step, the theoretical maxima of irradiation were extracted from the Solar Calculator tool available in MeteoExploration website [35]. The actual radiation maps, with a precision of 0.5°in both latitude and longitude were downloaded from the open database Global Solar Atlas [36], funded by the World Bank in order to help the development of sun-based technologies. The database provides data for direct normal irradiation (DNI), diffuse horizontal irradiation (DHI) and global horizontal irradiation (GHI). SODIS kinetics depend on the absorption of available photons, and its rate will depend on total incident radiation (TIR). To estimate this value, the direct normal incidence contribution (i.e., DNI) was added to the diffuse horizontal incidence contribution (i.e., DHI). As DHI is a measure of flux, considering the incidence angle of light, its contribution was doubled to obtain the associated incident radiation, considering isotropic distribution of diffuse light (Eq. (6)). Finally, instantaneous incident radiation was estimated from the yearly average data of daily accumulated doses using the average sun transit of 12 h (Eq (7)). Fig. 1 shows the distribution of the four magnitudes in Africa.

$$TIR = DNI + 2\ DHI \tag{6}$$

$$Instantaneous\ incident\ radiation = TIR\ /\ 12\ h \tag{7}$$

## 3. Results and discussion

### 3.1. Description of the experimental space and modeling of disinfection kinetics

Fig. 2 presents the results of the experiments, presenting various combinations of values indicated in the independent variables. More specifically, the various panels describe the experiments conducted in the dark (0 W/m$^2$, for the evaluation of thermal events), and at low (400 W/m$^2$), moderate (800 W/m$^2$) and maximum (simulated) sunlight intensity (1200 W/m$^2$). These irradiance levels represent values of solar light that are likely to be encountered over the course of a daily exposure of a sample to daylight in SODIS candidate countries. The chosen irradiance values correspond to approximately weak, moderate, and maximum light irradiance values reaching the Earth's surface. The operational conditions tested showed only small differences regarding organic matter and suspended solid levels, so we simplified the data and regrouped the results by temperature and irradiance; the vertical bars indicate the best and worst performance presented at each time, in a pseudo-confidence interval manner, within which the inactivation of microorganisms will lie (detailed presentation of the experiments is given in Supplementary Fig. S4).

Examining the effect of temperature up to almost 40 °C, we noted that the thermal effect was negligible. However, at 50 °C the process became thermally-driven and the inactivation of $10^6$ bacteria took place in under 4 h. Irradiation of the reactor enhanced the process. For instance, at the lower level of 400 W/m$^2$, the inactivation time decreased at water temperatures $\leq$ 40 °C, while at 50 °C the inactivation time was halved. Generally, for low(er) temperatures and low(er) irradiance values, the process is adequately represented by a line in logarithmic scale, with a minor slope, while at intermediate and high values, the process displays a distinct lag phase, followed by a linear phase. The synergies that appear for low irradiance values are clear, as well as the expected improvement at average and high irradiance values (800–1200 W/m$^2$). The observed synergies are related to a combination of thermal and solar-light mediated disinfection processes. Indeed, high temperature denatures protein structures affecting the stability of the cytoplasmic membrane as well as other enzymatic activities. The latter facilitates higher damage infliction by the solar light upon the cytoplasmic enzymes, hence the disinfection efficiency increases exponentially [37]. Furthermore, as radical recombination reactions have much lower thermal activation energies than radical attack reactions towards bacterial components, the higher the temperature, the higher the exploitation of radicals, and therefore the higher the optically-driven inactivation. Increasing sunlight intensity (800 W/m$^2$) produces enhanced inactivation at all water temperatures ($\geq$20 °C), which suggests that for the irradiance levels studied, there is a "solar threshold" above which solar-mediated inactivation of *E. coli* is effectively initiated. This process has been previously reported [38] and indicates the need to accumulate damage to inactivate the bacterial pathogens present in water. The reactors used in our study, as with SODIS containers typically used at household level, do not permit transmission of UVB irradiation [39], hence inactivation is a function of the internal oxidative damage initiated by inactivation of catalases, peroxidases and dismutases in the cell, initiating an internal photo-Fenton process, as published before [40,41]. However, we note once again, a faster inactivation of the microorganisms in the samples at high-temperature. Finally, high irradiance values (>800 W/m$^2$) showed that at low water temperatures, the process is optically-driven.

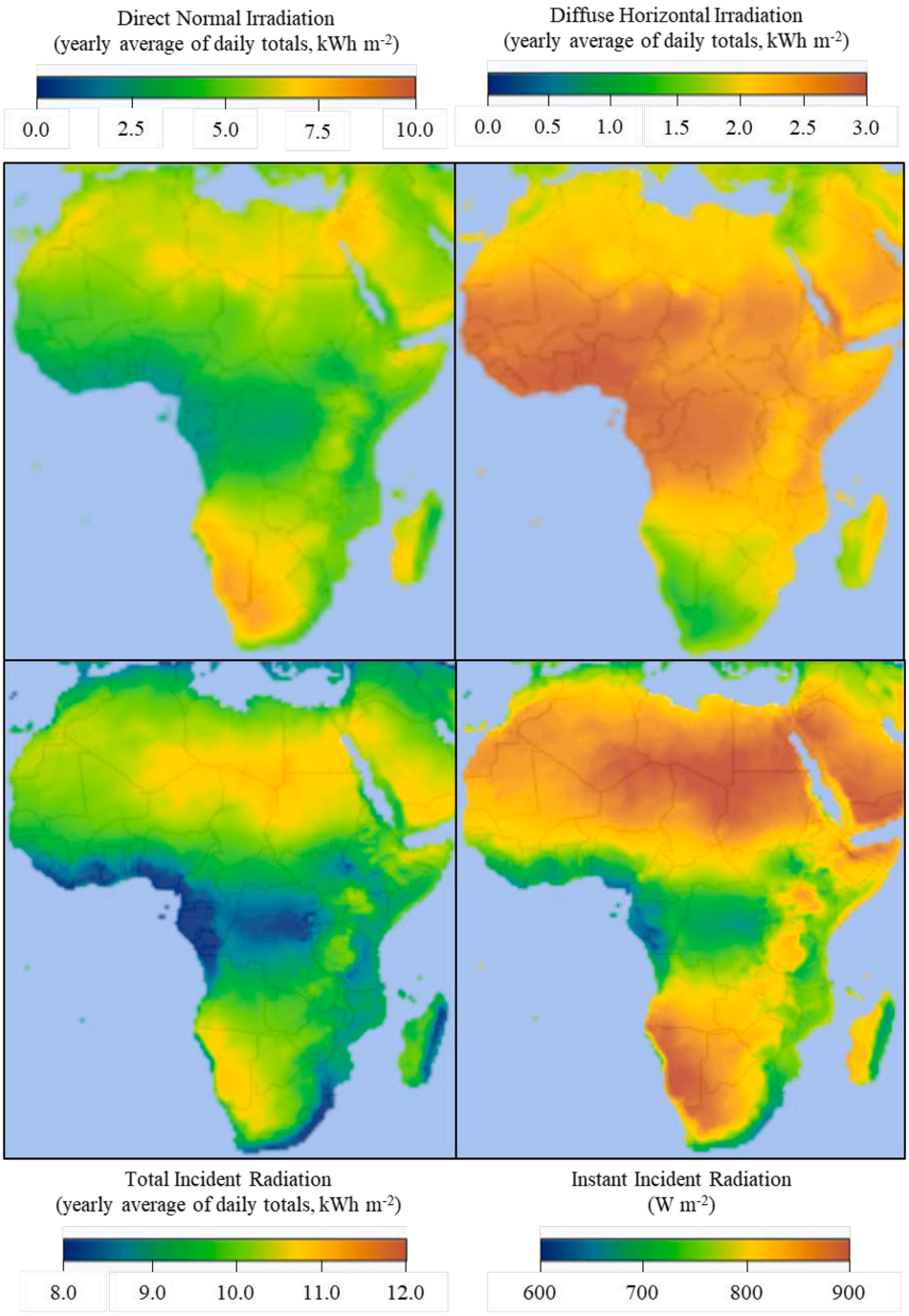


**Fig.1.** Distribution of incident radiation in Africa (data acquired from [36]).

From the above measurements, we confirm the dual nature of inactivation: optically-driven at low water temperature values and thermally driven for T > 40 °C. Synergy is observed in the range between these temperature limits [11]. However, at 50 °C the linear character of inactivation by thermal processes does not present a shoulder, thus confirming that heat is the main driving force of bacterial inactivation in these cases (see Fig. 2). Since, heat plays a crucial role with regard to vital cell components such as nucleic acid, the cell wall, proteins [42,43], this accelerated cell death is expected. Also noteworthy is the minimal variation in effect with irradiance levels from the four DOM/turbidity values tested at each temperature level (Fig. 2 - low/high DOM and low/high turbidity). More specifically, the optical inactivation is adversely affected by the presence of suspended solids and organic matter, while thermally driven processes are minimally affected.

The experimental data indicate that the process is adequately represented by a shoulder and/or a line (in log scale). As such, the model of Geeraerd and co-workers (Shoulder + log-linear fit) was assessed [22,24], and provide adequate descriptions of the process ($R^2$ always > 90%). The results are summarized in Fig. 3.

The applied disinfection modeling approach quantifies the initial observations, concerning the global evolution of the inactivation process, when irradiance and water temperatures increased. For instance, the inactivation rate (with *k* as its proxy) was almost constant in the 20 °C – 40 °C region, except for high irradiance values. Also, the increase of water temperature showed almost a linear effect on the lag phase of inactivation. It appears that the lack of optically sustained damage is replaced by the effect of heat. According to the literature, it is mainly thermally-mediated inactivation of catalases and superoxide

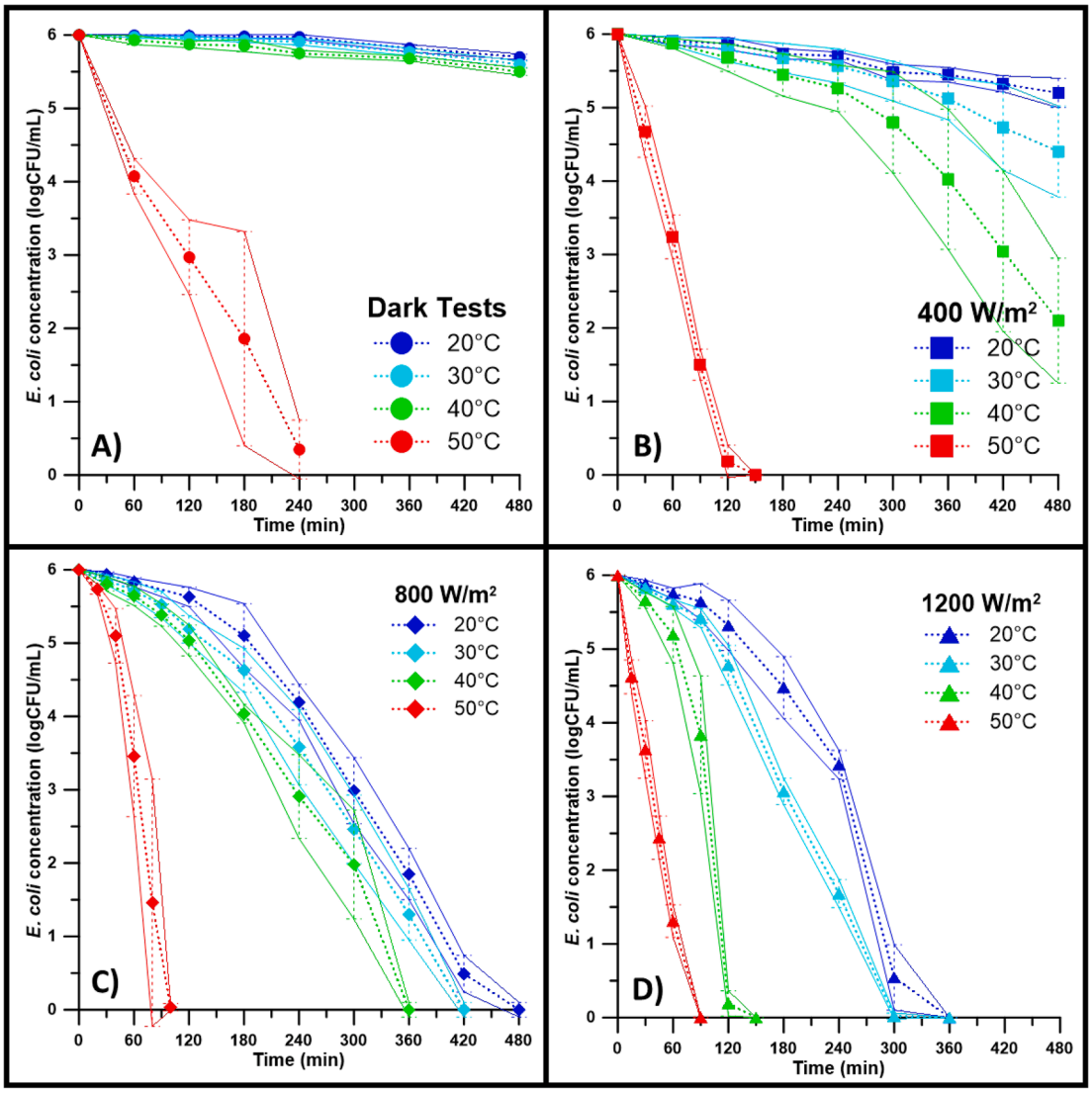


**Fig.2.** Bacterial inactivation under simulated solar/thermal treatment. A) Dark experiments (0 W/m$^2$). B) 400 W/m$^2$. C) 800 W/m$^2$ and D) 1200 W/m$^2$. The different colors indicate the water temperatures during the test. The plotted points are the average performance of the different conditions (aggregate of the 4 distinct cases) and the error bars indicate the highest/lowest inactivation noted for each set of conditions.

dismutases, that aggravate the internal oxidative stress and the subsequent damage inflicted by solar light [44]. Finally, the times required for inactivation are in reasonable agreement for both methods, with better statistical evaluation indices in the case of the shoulder log-linear approach (the detailed results of the statistical analyses for the two models are presented in Supplementary Table S1).

The results presented in Figs. 2 and 3 (and the respective supplementary material), indicate that the inactivation process could be represented as a function of the level of sunlight intensity provided to the sample and the prevailing water temperature conditions during treatment, over time. Hence, a model connecting the time necessary for inactivation with irradiance and temperature should be possible. As such, we proceeded to formulate a model where bacterial inactivation was set as a dependent variable with light intensity (irradiance) and temperature (I, T) set as independent variables. The candidate model should cover several climate conditions for the areas of potential of interest, while taking into account the effect of latitude/longitude changes around SODIS candidate regions.

Incorporating the model will allow prediction of bacterial inactivation, and the statistical analysis will provide insight into the importance the factors implicated, such as light and water temperature, as well as their interaction effect as independent variables. Furthermore, the dependence of inactivation on these factors will be characterized according to their relationship. To this end, static and dynamic modeling of bacterial inactivation will be further assessed.

### *3.2. Predicting solar disinfection: static and dynamic bacterial inactivation modeling*

#### *3.2.1. Static modeling of bacterial inactivation*

A stochastic approach is hereby proposed that assesses bacterial inactivation by solar-assisted processes. The objective is to understand the relationship between bacteria and the conditions that affect their dynamics, hence regression models with static and dynamic expressions are introduced as an unbiased and repeatable method. Bacterial inactivation (in logarithmic scale) is selected as a representative response variable, as it is monotonic and could provide an unambiguous conclusion regarding their potential association with sunlight intensity and temperature over time.

The objective of the static model is to predict bacterial inactivation under several climatic conditions. For this the experimental data of several water temperature levels, intensities, water compositions and

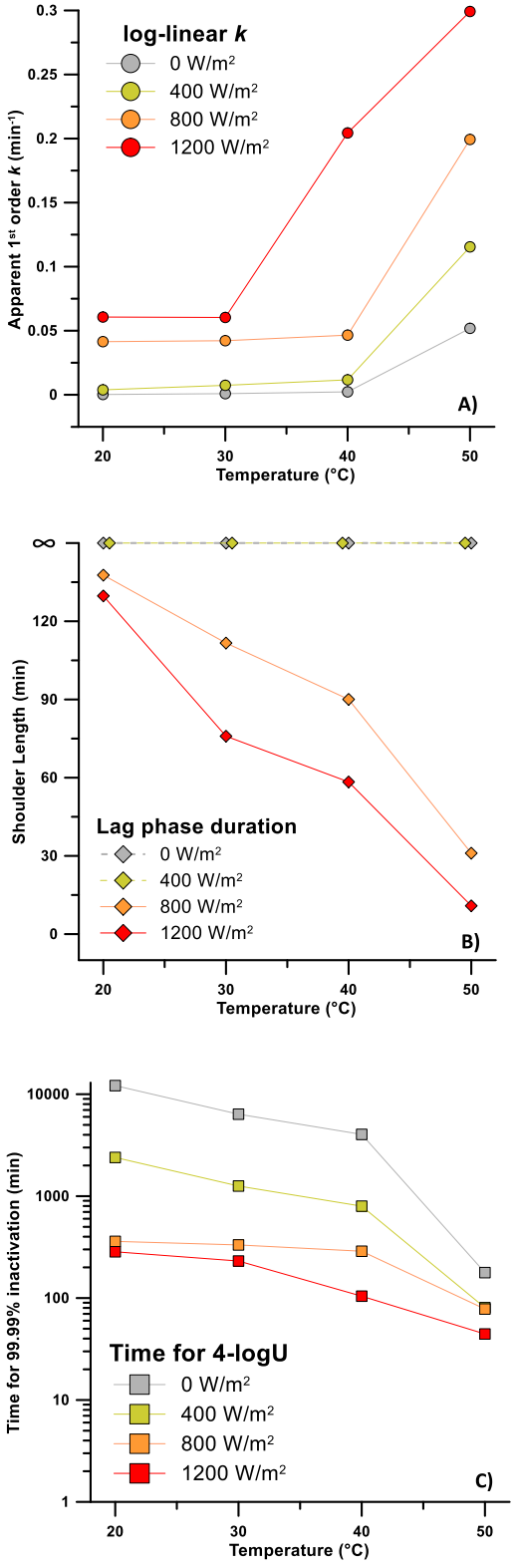


**Fig.3.** Bacterial inactivation model parameters and necessary time for 4 log bacterial inactivation for each process, at the water temperature levels tested in the solar/thermal treatment (20–50 °C). A) k constant. B) Lag phase duration (Sl). C) Time for 99.99% (4-log) elimination of *E. coli*. The different colors indicate the various irradiance values of the tests (0–1200 W/m$^2$). Note the "infinite" shoulder at 0 and 400 W/m$^2$ of panel B, at irradiance values which are adequately described by log-linear fitting and the logarithmic scale of Y-axis in panel C.

other environmental conditions that are described in the previous subsection (3.1) are modelled.

To develop the proposed model, statistics of the linear combination of variables (time, temperature, sunlight intensity, DOM and turbidity) were studied, as well as combinations of linear and squared terms of the same variables. Those terms with the highest p-values were selected, in an attempt to achieve a balance between the model's ability to predict the experimental data, and the number of parameters in the model. Tables S2 and S3 in the supplementary material show the results of the statistical analysis.

The conception of the proposed model is based on the effect that the interactions of the synergistic solar/thermal factor and the thermal factor have on bacterial cultivability. This concept is formulated in Equation (8):

$$Inactivation = Synergistic\ Solar/Thermal\ Effect + Thermal\ Effect \quad (8)$$

The formulation suggests that a thermal effect can independently lead to bacterial inactivation, while in real applications solar light may imply an increase in water temperature, hence always acting simultaneously, while the effect of DOM and SS at the levels tested were found to be negligible and were not considered further. An initial approach to model this concept resulted in a static model. The logarithm of bacterial inactivation, or *logInact*, is assigned as a response variable, in order to capture the dynamics relying on the behavior of the bacteria after exposure to heat $T$ and intensity $I$, which describe the *logInact* and refer to current time instance $t$. The coefficients of the variables are denoted by $\beta_i$. The intercept of the model is set to 0, as at time $t = 0$ the bacterial inactivation should be 0.

Although this model had statistically significant interactions between intensity, water temperature, and time ($I \times T \times t$ and T × t), which have a physical meaning in explaining inactivation, it did not sufficiently describe the observations' observed within the experimental space (Supplementary Table S2). As such, a higher order model was required (Supplementary Table S3). The second order variables that were introduced into the independent variables' interactions were meant to better describe the hyperplane of the experimental space. Indeed, this model created a better fit to the data, with the $R^2_{adj}$ increasing from 0.7386 to 0.8784. It should be noted that the $R^2_{adj}$ adjusts to the number of independent variables, increasing only by the decrease of the residual variance, and not by the increase of the number of variables that are included in the model. Nevertheless, apart from the independent variables' interactions that reflect the conceptual base of the model ($I^2 \times T \times t$ and $T^2 \times t$) and appear statistically significant, the remaining interactions and variables are either statistically insignificant or without physical meaning. Consequently, the explanation of 87.8% of the variance found in the bacterial inactivation by an increased number of high and lower order terms is reasonable.

Consequently, the static model that we propose is the most minimally adequate model that plays a dual role; it includes variables reflecting the hypothesis - namely the thermal and solar/thermal influence factors - and maintains statistically significant variables with physical meanings. The model, the summary of linear output and the statistical performance evaluation are presented in Table 3.

Based on $n = 420$ observations, both the solar/thermal and the thermal independent variables' interactions positively affect bacterial inactivation (counted in logarithmic units). An increase in any of the two interactions indicates an increase in bacterial inactivation. For example, for a day with very good SODIS conditions (water temperature $T = 30^oC$ and intensity $I = 800\ W/m^2$) and for $t = 300\ min$ the bacterial inactivation based on the estimated $\beta$ coefficients would be $4.3 \times 10^{-6} \times 800^2 \times 30 \times 300 + 3.8 \times 10^{-10} \times 30^2 \times 300 = 24768$ CFU/mL.

Regarding the statistical significance of the two explanatory variables, high *P-values* indicate that the relationship between the variables representing the solar/thermal and thermal interactions and the bacterial inactivation, is not based on chance since the null hypothesis can be

**Table 3**
Proposed static prediction model summary and statistical performance evaluation.

$Y_{logInact_{(t)}} = \beta_{I^2:T:t}\left(X_{I^2}X_TX_t\right)_{(t)} + \beta_{T^2:t}\left(X_{T^2}X_t\right)_{(t)}$

| Variable's name | Coefficient estimate$\beta$ | Std. Error | P-value | Confidence level* |
|---|---|---|---|---|
| $Y_{logInact_{(t)}}$ | (n = 420) | | | |
| $\beta_{I^2:T:t}$ | $3.8 \times 10^{-10}$ | $2.2 \times 10^{-11}$ | $< 2 \times 10^{-16}$ | 99.9% |
| $\beta_{T^2:t}$ | $4.3 \times 10^{-6}$ | $3.5 \times 10^{-7}$ | $< 2 \times 10^{-16}$ | 99.9% |
| RSE | 1.168 | | | |
| $R^2$-adjusted | 0.717 | | | |
| * based on *t*-test | | | | |

* based on *t*-test

rejected with a confidence level of 99.9% for both interactions.

Based on the statistical assessment, the static approach adequately models the bacterial inactivation, yielding good fits (71.7%) and high accuracy (1.168). The high value of the adjusted $R^2$, which does not increase with every independent variable involved in the model as the $R^2$, suggests that the proportion of total observed variance in bacterial inactivation explained by the model, is considerably better than that resulting from a naïve model. More explicitly, approximately 72% of the variance of bacterial inactivation can be explained by the model's two main interactions of solar/thermal and thermal effect. The low residual standard error (RSE) denotes that the model predicts bacterial inactivation with a low error of $\pm$ 1.168 in logarithmic units on 418 degrees of freedom. Namely, 418 observations were used for the estimation, with only 2 variables as restriction.

Furthermore, the independent variables are examined for multicollinearity, as inter-correlation between these variables would inflate in absolute terms the estimated coefficients, variances and standard errors, and would result in the bias of the significance tests that depend on the aforementioned. Analysis of the Variance inflation factor (VIF)[2] for the two involved independent variables, resulted in both being equal to 1.51. This suggests that the variables are minimally correlated, hence the regression results are strongly reliable. Consequently, the proposed model can be used to estimate inactivation for most of the climatic conditions encountered in SODIS candidate countries.

### 3.2.2. *Dynamic modeling of bacterial inactivation*

To describe and predict the likely bacterial inactivation dynamics over time, a dynamic multivariate linear regression model is next proposed. To capture the spatio-temporal patterns in bacterial inactivation under similar circumstances as in the static model's case (subsection 3.3.1), the same variables are assessed. An additional explanatory variable is added to the model, to provide a time-varying, dynamic approach. This is the time-lagged variable of bacterial inactivation one time-step prior $(t-1)$ to the currently observed (in time t) bacterial inactivation. This is based on the rationale that the bacterial inactivation one time-step prior to the current step, affects the current bacterial inactivation. Hence, the time-lagged explanatory variable accounts for time variations. Fig. 4 summarizes the change in the computational approach.

Predicting of bacterial inactivation at time $t$ is a function of the bacterial concentration at time $t-1$ and the prevailing environmental

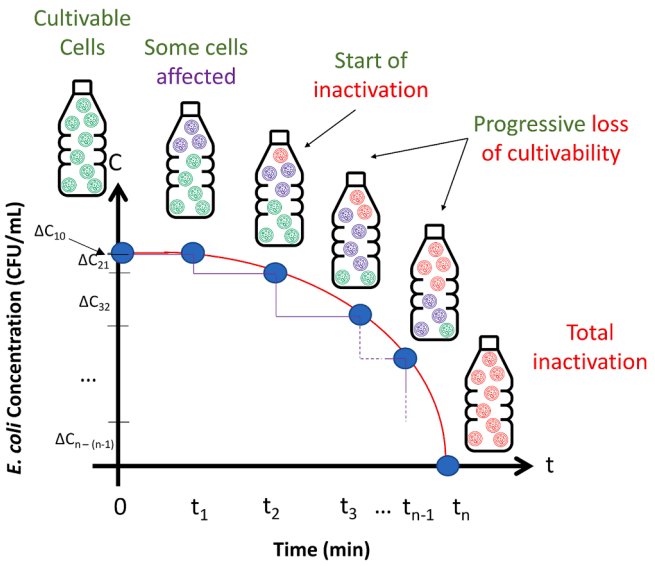


**Fig.4.** Dynamic modeling approach: the concentration of bacteria at each time point is the concentration at the previous point reduced by the inactivation that took place in time Δt. The reactors initially contain only cultivable cells (green), for as long as the shoulder period lasts the cells sustain damage, but no inactivation occurs (purple cells), then inactivation starts (red cells), down to the point where total inactivation is achieved (with the possibility of having viable but not cultivable cells).

conditions of intensity and water temperature from time $t-1$ until time $t$. The prediction horizon is set on one time-step, which is considered sufficient to detect essential changes (i.e., decay), without missing or accentuating any rapid fluctuations caused by growth or other adaptation-related biological events. A short forecasting horizon is required, in order to maintain acceptable prediction accuracy and interpretable predictions.

This dynamic approach is described by the dynamic regression model presented in Table 4 that describes bacterial inactivation dynamics across all climatic conditions considered with the indicators of water temperature and intensity over time, similarly to the static approach presented in Table 4. The statistical performance evaluation is presented in the same table. It is noted that the dynamic model corresponding to the second initial static prediction model, was also tested (Supplementary Table S4). However, similarly to the static approach, the lower order interactions and independent variables were without interactions and were statistically insignificant or without physical meaning, so no further analysis deems necessary.

Both the solar/thermal and thermal factors represented by the

**Table 4**
Proposed dynamic prediction model summary and statistical performance evaluation.

$Y_{logInact_{(t)}} = \varphi_{logInact}Y_{logInact_{(t-1)}} + \beta_{I^2:T:t}\left(X_{I^2}X_TX_t\right)_{(t)} + \beta_{T^2:t}\left(X_{T^2}X_t\right)_{(t)}$

| Variable's name | Coefficient estimate$\beta$ | Std. Error | P-value | Confidence level* |
|---|---|---|---|---|
| $Y_{logInact_{(t)}}$ | (n = 420) | | | |
| $\varphi_{logInact_{(t-1)}}$ | 1.127 | 0.036 | $< 2 \times 10^{-16}$ | 99.9% |
| $\beta_{I^2:T:t_{(t)}}$ | $1.3 \times 10^{-10}$ | $1.4 \times 10^{-11}$ | $< 2 \times 10^{-16}$ | 99.9% |
| $\beta_{T^2:t_{(t)}}$ | $9.8 \times 10^{-7}$ | $2.2 \times 10^{-7}$ | $7.7 \times 10^{-6}$ | 99.9% |
| RSE | 0.635 | | | |
| $R^2$-adjusted | 0.916 | | | |

* based on *t*-test

[2] The variance inflation factor analysis is computed as the ratio of the sum of squared residual errors over the native variance of the variables, for n and not n-1 respecting the intercept 0. For factors' values lower or equal to 1 the variables are not correlated, for 1 to 5 they are moderately correlated, and for values>5 are highly correlated.

explanatory variables' interactions (of the squared intensity with temperature and time, and of the squared temperature with time), show the same behavior as in the static model, as was expected. More precisely, an increase in $I^2 \times T \times t$ or $T^2 \times t$ indicates that in the forthcoming time step the bacterial inactivation will increase by the corresponding logarithmic values. So in a day with known or well-estimated water temperature and intensity conditions, the model can predict the bacterial inactivation of the forthcoming time step after a specific time period of exposure to light and the value lagged by one time step of bacterial inactivation ($logInact(t-1)$).

All independent variables are statistically significant, and the null hypothesis can be rejected with a confidence level of 99.9%. This statistical assessment demonstrates that the dynamic approach of the proposed model adequately predicts bacterial inactivation at logarithmic scale at one time step subsequent to the current, with very good fitting (91.6%) and high accuracy (0.635). The high adjusted $R^2$ indicates that 91.6% is the proportion of variance of bacterial inactivation at time $t$ that is explained by the proposed model, which is significantly better than the variance that would result from a naïve model. Furthermore, the model predicts the aforementioned bacterial inactivation with a low error of $\pm$ 0.635 on 417 degrees of freedom, as only 3 variables out of the 420 observations are set as restrictions, being the independent variables.

The Variance inflation factor (VIF) analysis for the two independent variables' interactions suggests that the variables are minimally correlated, as the values are 2.20 and 1.97 for the solar/thermal and the thermal variables, respectively. For example, the VIF of the $I^2 \times T \times t$ variable indicates that the standard error for the coefficient of that variable is $\sqrt{2.2} = 1.48$ times more inflated than if the variable had zero correlation with the other dependent variables. Given the small coefficient of the $I^2 \times T \times t$ variable, produces a coefficient that is larger in the 11th decimal ($\beta_{I^2:T:t_{(t)}}$ should be $1.9 \times 10^{-10}$ instead of $1.3 \times 10^{-10}$). This means that the error has little effect on the prediction of bacterial inactivation. Even for the time-lagged variable, the VIF of 2.8 does not indicate a multi-collinearity issue. The above observations suggest that the regression results are very reliable.

As a provisional conclusion, we propose that the introduced dynamic model reliably describes and predicts bacterial inactivation across the numerous climatic conditions encountered in several countries, where SODIS application is or can be potentially applied. Furthermore, the synergy between the actions of the dual nature of light (photons, heat) is successfully captured by the statistically significant variables included in the model, which represent the solar/thermal and thermal factors and explain the bacterial inactivation.

### 3.3. *In silico* prediction of SODIS efficiency: application in Africa as a case study

In this section, based on the experimental results acquired and the produced models, we attempt to predict the likely bacterial inactivation across the African continent. Africa was selected as a case study, because high irradiance values and high water temperatures have been encountered during solar disinfection of surface and groundwater [45–48]. The irradiation corresponding to clear, cloudless skies, with uninterrupted irradiation, the yearly distribution of the theoretical maximum of sunlight intensity, as a function of the latitude, is depicted in Figure S5 with representative locations in South Africa and along the Rift Valley (Malawi, Uganda and Ethiopia).

The irradiation profiles and thresholds indicate that most of the sites could theoretically achieve total inactivation, based on the results acquired in the disinfection experiments. For instance, in Uganda, the calculation suggests a minimum of 8 h available over the 400 W/m$^2$ threshold (min. irradiance in which inactivation took place in lab tests), hence SODIS could be effectively applied all year round.

However, the actual local irradiance conditions greatly affect the possibility of SODIS application in Africa and have to be considered in the calculations and forecast of SODIS efficacy. Fig. 5 shows disinfection maps generated for Africa using the predictions of the inactivation models, based on the estimated yearly average values of temperature and actual (not theoretical) incident radiation from respective databases. Values of exposure time were calculated for a 4-log target inactivation of *E. coli* using the static model (Fig. 5A) and the dynamic model (Fig. 5B).

The static model leads to a better description of the SODIS process potential based on yearly averaged values of irradiance and temperature. In contrast, the dynamic model provides a better prediction of the disinfection performance if instantaneous experimental values of temperature and radiation (or hourly weather forecast) are available.

The results of the static model (Fig. 5A) confirm that the required inactivation time is mostly below the standard value of six hours, apart from the most meridional latitudes in South Africa and the Rift Valley (i.e. region around Tanzania, Kenya, Ethiopia). This effect is attributed to the existence of higher overall cloud-cover and lower ambient temperatures in the greener/wetter equatorial regions, and also the effect of higher temperature in the Sahara, Namibia, Kalahari, and Nubian deserts.

Fig. 5B shows the predictions of the dynamic model. In this case, although the values of temperature and irradiance are in the range used for the fitting of the model, in most cases the level of inactivation of 4-log requires exposure time beyond the 8 h. This is due to the use of a logarithmic response variable with a higher-order model increases the uncertainty in the extrapolation of the model for *in silico* predictions, especially considering the non-linear nature of the time dependence of the model. As such, the model over-estimates the time necessary for exposure, given the aggregated, annual averages. However, if one knows the weather conditions at a smaller scale (e.g., monthly; see Figures S6A and S6B for July and January predictions respectively), the prediction becomes much more accurate. Furthermore, by applying this in a time horizon of one day, the model could provide sufficient prediction of the bacterial inactivation via SODIS, a more precise prediction than can be achieved using calendar months are obtained. A model such as the one presented here would allow the definition of a reliable and efficient *a priori* protocol to SODIS disinfect water according to the prevailing environmental conditions. Thus, this model represents a milestone towards an easier and more cautious (and hence safer) implementation of SODIS in those areas that lack facilities to treat water resources.

## 4. Conclusions

In this work, the prediction of SODIS efficacy was attempted to be made, based on the measured inactivation rates under laboratory conditions. This has led to the following conclusions:

- The design of experiments chosen represents well water that is intrinsically clearer (e.g. groundwater) or that has undergone a filtration/sedimentation, even a rudimentary one. This results in low values of turbidity (<50 NTU) and DOM quantities (6 mg/L). The inactivation was achieved well within the timeframe of 6-h exposure and the kinetic constants describing the inactivation were well correlated with water temperature and irradiance values.
- Temperature has been found to greatly enhance inactivation and is the main driving force in the absence of sunlight or for irradiance values<800 W/m$^2$. At the upper range of water temperatures tested, inactivation occurred with lower irradiance values as well. Hence, in order to ensure efficacy, optical and thermal thresholds should be considered.
- The static and dynamic models introduced describe and successfully predict bacterial inactivation under numerous global climatic conditions. This is reinforced by the models' predictive performance which has significant prediction certainty, namely low residual standard errors (1.168 and 0.635 respectively). Furthermore, the

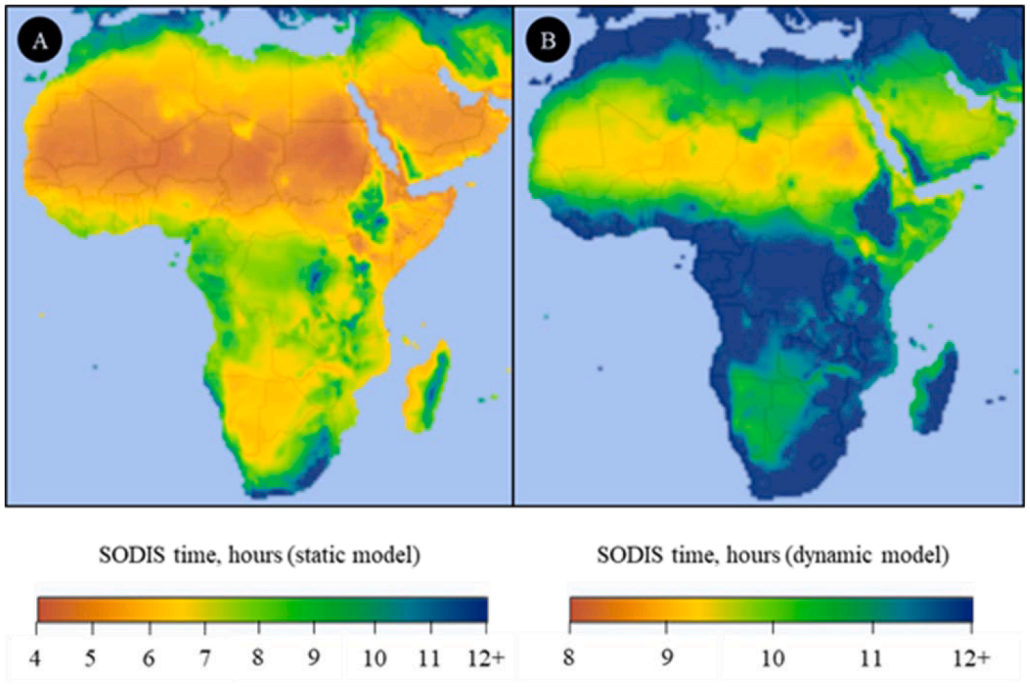


**Fig.5.** SODIS time required to achieve a 4-log inactivation in Africa using both proposed models, static and dynamic formulations.

variance inflation analyses for the independent variables of both models suggest that there is no multi-collinearity issue, so predictive strength is not compromised.

- Introducing realistic field values of cloud coverage, incident irradiation and ambient temperature leads to an estimation of the time necessary for solar exposure in order to acquire safe water according to WHO (4-logU bacterial inactivation). The static model performed better in the ranges tested in the lab, while the dynamic model overestimates the times necessary, albeit at a fail-safe range.
- Application of the models in Africa produced a valuable map of the times necessary for SODIS exposure to inactivate 4-logU (99.99%) of the bacterial concentration in water, which could act as a guideline or a policy implementation tool for SODIS applications in the continent.

Nevertheless, we believe that we should draw attention to the following matters which may affect real applications. To allow for the possibility of using highly contaminated water sources, as is often the case in water scarce regions, any future design should further explore turbidity values as high as 200–300 NTU and DOM up to 10–15 mg/L. Secondly, although the models fitted the inactivation well, it is crucial to more mechanistic aspects related with bacterial inactivation (e.g. DNA damage, enzyme inactivation, specific thermal effects). Future steps in dynamic modeling should incorporate these constantly time-varying elements as well as the evolution of the total bacterial concentration. Finally, the addition of chemical matrix effects in indirect pathways of bacterial inactivation should also be considered; besides direct UV/thermal actions, the generation of transient and photo-induced reactive species should be contemplated at least at lab scale. Furthermore, an assessment of the eventual by-products generated during SODIS may help to better evaluate the safety of the final water matrix for practical applications. The intrinsic difficulties of precise measurements in the SODIS regions should be compensated by the highest level possible of laboratory precision.

## Declaration of Competing Interest

The authors declare that they have no known competing financial interests or personal relationships that could have appeared to influence the work reported in this paper.

## Acknowledgements

Cesar Pulgarin, Kevin McGuigan and Javier Marugán would like to acknowledge the financial support through the European project WATERSPOUTT H2020-Water-5c-2015 (GA 688928) and the Swiss State Secretariat for Education, Research and Innovation (SEFRI-WATERSPOUTT, No.: 588141). Stefanos Giannakis acknowledges the Spanish Ministry of Science, Innovation and Universities (MICIU) for the Ramón y Cajal Fellowship (RYC2018-024033-I).

## Appendix A. Supplementary data

Supplementary data to this article can be found online at https://doi.org/10.1016/j.cej.2021.130866.

## References

[1] W.H.O., World Health Organization, WHO International Scheme to Evaluate Household Water Treatment Technologies Harmonized Testing Protocol, Technology Non-Specific. (2014).
[2] K.G. McGuigan, R.M. Conroy, H.J. Mosler, M. du Preez, E. Ubomba-Jaswa, P. Fernandez-Ibañez, P. Fernandez-Ibanez, Solar water disinfection (SODIS): a review from bench-top to roof-top, J Hazard Mater. 235–236 (2012) 29–46, https://doi.org/10.1016/j.jhazmat.2012.07.053.
[3] S. Giannakis, E. Darakas, Antoni Escalas-Cañellas, César Pulgarin, Environmental considerations on solar disinfection of wastewater and the subsequent bacterial (re)growth, Photochem. Photobiol. Sci. 14 (3) (2015) 618–625, https://doi.org/10.1039/C4PP00266K.
[4] M. Berney, H.-U. Weilenmann, A. Simonetti, T. Egli, Efficacy of solar disinfection of Escherichia coli, Shigella flexneri, Salmonella Typhimurium and Vibrio cholerae, J Appl Microbiol. 101 (4) (2006) 828–836, https://doi.org/10.1111/jam.2006.101.issue-410.1111/j.1365-2672.2006.02983.x.
[5] F. Bosshard, M. Bucheli, Y. Meur, T. Egli, The respiratory chain is the cell's Achilles' heel during UVA inactivation in Escherichia coli, Microbiology. 156 (2010) 2006–2015.
[6] M. Castro-Alférez, M.I. Polo-López, P. Fernández-Ibáñez, Intracellular mechanisms of solar water disinfection, Sci. Rep. 6 (2016) 38145.
[7] K. Keyer, J.A. Imlay, Superoxide accelerates DNA damage by elevating free-iron levels, Proc. Natl. Acad. Sci. 93 (24) (1996) 13635–13640.
[8] S. Giannakis, M. Voumard, S. Rtimi, C. Pulgarin, Bacterial disinfection by the photo-Fenton process: Extracellular oxidation or intracellular photo-catalysis?

Appl. Catal. B Environ. 227 (2018) 285–295, https://doi.org/10.1016/j.apcatb.2018.01.044.
[9] L. Feng, C. Peillex-Delphe, C. Lü, D. Wang, S. Giannakis, C. Pulgarin, Employing bacterial mutations for the elucidation of photo-Fenton disinfection: Focus on the intracellular and extracellular inactivation mechanisms induced by UVA and H2O2, Water Res. 182 (2020), 116049, https://doi.org/10.1016/j.watres.2020.116049.
[10] M. Castro-Alférez, M.I. Polo-López, J. Marugán, P. Fernández-Ibáñez, Mechanistic model of the Escherichia coli inactivation by solar disinfection based on the photo-generation of internal ROS and the photo-inactivation of enzymes: CAT and SOD, Chem. Eng. J. 318 (2017) 214–223.
[11] K.G. McGuigan, T.M. Joyce, R.M. Conroy, J.B. Gillespie, M. Elmore-Meegan, Solar disinfection of drinking water contained in transparent plastic bottles: characterizing the bacterial inactivation process, J Appl Microbiol. 84 (1998) 1138–1148.
[12] M. Castro-Alférez, M.I. Polo-López, J. Marugán, P. Fernández-Ibáñez, Mechanistic modeling of UV and mild-heat synergistic effect on solar water disinfection, Chem. Eng. J. 316 (2017) 111–120.
[13] M. Castro-Alférez, M. Inmaculada Polo-López, J. Marugán, P. Fernández-Ibáñez, M. I. Polo-López, J. Marugán, P. Fernández-Ibáñez, Validation of a solar-thermal water disinfection model for Escherichia coli inactivation in pilot scale solar reactors and real conditions, Chem. Eng. J. 331 (2018) 831–840, https://doi.org/10.1016/j.cej.2017.09.015.
[14] E.A. Serna-Galvis, J.A. Troyon, S. Giannakis, R.A. Torres-Palma, L. Carena, D. Vione, C. Pulgarin, Kinetic modeling of lag times during photo-induced inactivation of E. coli in sunlit surface waters: Unraveling the pathways of exogenous action, Water Res. 163 (2019), 114894.
[15] R.J. Davies-Colley, C.W. Hickey, J.M. Quinn, Organic matter, nutrients, and optical characteristics of sewage lagoon effluents, New Zeal. J. Mar. Freshw. Res. 29 (2) (1995) 235–250.
[16] S.C. Kehoe, T.M. Joyce, P. Ibrahim, J.B. Gillespie, R.A. Shahar, K.G. McGuigan, Effect of agitation, turbidity, aluminium foil reflectors and container volume on the inactivation efficiency of batch-process solar disinfectors, Water Res. 35 (2001) 1061–1065.
[17] E. Ubomba-Jaswa, C. Navntoft, M.I. Polo-López, P. Fernandez-Ibáñez, K. G. McGuigan, Solar disinfection of drinking water (SODIS): an investigation of the effect of UV-A dose on inactivation efficiency, Photochem. Photobiol. Sci. 8 (2009) 587–595, https://doi.org/10.1039/b816593a.
[18] R. Khaengraeng, R.H. Reed, Oxygen and photoinactivation of Escherichia coli in UVA and sunlight, J Appl Microbiol 99 (1) (2005) 39–50.
[19] M. Marjanovic, S. Giannakis, D. Grandjean, L.F. de Alencastro, C. Pulgarin, Effect of MM Fe addition, mild heat and solar UV on sulfate radical-mediated inactivation of bacteria, viruses, and micropollutant degradation in water, Water Res. 140 (2018) 220–231, https://doi.org/10.1016/j.watres.2018.04.054.
[20] M. Fabbricino, L. d'Antonio, Use of solar radiation for continuous water disinfection in isolated areas, Environ. Technol. 33 (5) (2012) 539–544, https://doi.org/10.1080/09593330.2011.584570.
[21] L.F. Caslake, D.J. Connolly, V. Menon, C.M. Duncanson, R. Rojas, J. Tavakoli, Disinfection of Contaminated Water by Using Solar Irradiation, Appl. Environ. Microbiol. 70 (2) (2004) 1145–1151, https://doi.org/10.1128/AEM.70.2.1145-1150.2004.
[22] A.H. Geeraerd, V.P. Valdramidis, J.F. Van Impe, GInaFiT, a freeware tool to assess non-log-linear microbial survivor curves, Int. J. Food Microbiol. 102 (1) (2005) 95–105.
[23] O.K. Dalrymple, E. Stefanakos, M.A. Trotz, D.Y. Goswami, A review of the mechanisms and modeling of photocatalytic disinfection, Appl. Catal. B Environ. 98 (1-2) (2010) 27–38.
[24] A.H. Geeraerd, C.H. Herremans, J.F. Van Impe, Structural model requirements to describe microbial inactivation during a mild heat treatment, Int. J. Food Microbiol. 59 (3) (2000) 185–209.
[25] S. Giannakis, S. Watts, S. Rtimi, C. Pulgarin, Solar light and the photo-Fenton process against antibiotic resistant bacteria in wastewater: A kinetic study with a Streptomycin-resistant strain, Catal. Today. 313 (2018) 86–93, https://doi.org/10.1016/j.cattod.2017.10.033.
[26] S. Giannakis, E. Darakas, A. Escalas-Cañellas, C. Pulgarin, Solar disinfection modeling and post-irradiation response of Escherichia coli in wastewater, Chem. Eng. J. 281 (2015) 588–598, https://doi.org/10.1016/j.cej.2015.06.077.
[27] J. Rodríguez-Chueca, M.P. Ormad Melero, R. Mosteo Abad, J. Esteban Finol, J. L. Ovelleiro Narvión, Inactivation of Escherichia coli in fresh water with advanced oxidation processes based on the combination of O3, H2O2, and TiO2. Kinetic modeling, Environ. Sci. Pollut. Res. 22 (2015) 10280–10290, https://doi.org/10.1007/s11356-015-4222-3.
[28] J. Rodríguez-Chueca, M.P. Ormad, R. Mosteo, S. Canalis, J.L. Ovelleiro, Escherichia coli Inactivation in Fresh Water Through Photocatalysis with TiO2-Effect of H2O2on Disinfection Kinetics, Clean - Soil, Air, Water. 44 (5) (2016) 515–524, https://doi.org/10.1002/clen.v44.510.1002/clen.201500083.
[29] W. Harm, Biological effects of ultraviolet radiation, Cambridge University Press Cambridge, 1980.
[30] A. Argoti, R.G. Maghirang, A.F. González Barrios, S.T. Chou, L.T. Fan, A generalized model for bacterial disinfection: Stochastic approach, Biochem. Eng. J. 114 (2016) 218–225.
[31] E. Rommozzi, S. Giannakis, R. Giovannetti, D. Vione, C. Pulgarin, Detrimental vs. beneficial influence of ions during solar (SODIS) and photo-Fenton disinfection of E. coli in water: (Bi)carbonate, chloride, nitrate and nitrite effects, Appl. Catal. B Environ. 270 (2020), 118877, https://doi.org/10.1016/j.apcatb.2020.118877.
[32] S. Samoili, G. Farinelli, J. Moreno-SanSegundo, G. Stefanos, K. McGuigan, J. Marugán, C. Pulgarín, Dataset: SODIS performance on the inactivation of E, in: coli under different irradiance and temperature conditions, 2020, https://doi.org/10.5281/ZENODO.4277905.
[33] WHO, International Scheme to Evaluate Household Water Treatment Technologies Harmonized Testing Protocol, Technology Non-Specific Version 2 (2018) 1.
[34] P. Valero, S. Giannakis, R. Mosteo, M.P. Ormad, C. Pulgarin, Comparative effect of growth media on the monitoring of E. coli inactivation and regrowth after solar and photo-Fenton treatment, Chem. Eng. J. 313 (2017) 109–120, https://doi.org/10.1016/j.cej.2016.11.126.
[35] SolarCalc, Solar Calculator Tool - Meteoexploration.com, (2020). https://meteoexploration.com/products/SolarCalculator.html (accessed October 9, 2020).
[36] SOLARGIS, ESMAP, SOLARGIS, WB, IFC, Https://Globalsolaratlas.Info/Map. (2019).
[37] S. Giannakis, Analogies and differences among bacterial and viral disinfection by the photo-Fenton process at neutral pH: a mini review, Environ. Sci. Pollut. Res. 25 (28) (2018) 27676–27692, https://doi.org/10.1007/s11356-017-0926-x.
[38] J. Ndounla, S. Kenfack, J. Wéthé, C. Pulgarin, Relevant impact of irradiance (vs. dose) and evolution of pH and mineral nitrogen compounds during natural water disinfection by photo-Fenton in a solar CPC reactor, Appl. Catal. B Environ. 148–149 (2014) 144–153, https://doi.org/10.1016/j.apcatb.2013.10.048.
[39] P. Ozores Diez, S. Giannakis, J. Rodríguez-Chueca, D. Wang, B. Quilty, R. Devery, K. McGuigan, C. Pulgarin, Enhancing solar disinfection (SODIS) with the photo-Fenton or the Fe2+/peroxymonosulfate-activation process in large-scale plastic bottles leads to toxicologically safe drinking water, Water Res. 186 (2020) 116387, https://doi.org/10.1016/j.watres.2020.116387.
[40] S. Giannakis, M.I. Polo López, D. Spuhler, J.A. Sánchez Pérez, P. Fernández Ibáñez, C. Pulgarin, Solar disinfection is an augmentable, in situ-generated photo-Fenton reaction—Part 1: A review of the mechanisms and the fundamental aspects of the process, Appl. Catal. B Environ. 199 (2016) 199–223, https://doi.org/10.1016/j.apcatb.2016.06.009.
[41] S. Giannakis, M.I.P. López, D. Spuhler, J.A.S. Pérez, P.F. Ibáñez, C. Pulgarin, Solar disinfection is an augmentable, in situ-generated photo-Fenton reaction-Part 2: A review of the applications for drinking water and wastewater disinfection, Appl. Catal. B Environ. 198 (2016) 431–446, https://doi.org/10.1016/j.apcatb.2016.06.007.
[42] R.A. Blaustein, Y. Pachepsky, R.L. Hill, D.R. Shelton, G. Whelan, Escherichia coli survival in waters: Temperature dependence, Water Res. 47 (2) (2013) 569–578, https://doi.org/10.1016/j.watres.2012.10.027.
[43] P. Chakraborty, A Textbook of Microbiology, New Central Book Agency, 2005.
[44] M.B. Fisher, K.L. Nelson, Inactivation of Escherichia coli by Polychromatic Simulated Sunlight: Evidence for and Implications of a Fenton Mechanism Involving Iron, Hydrogen Peroxide, and Superoxide, Appl. Environ. Microbiol. 80 (2014) 935–942.
[45] R. Nalwanga, B. Quilty, C. Muyanja, P. Fernandez-Ibañez, K.G. McGuigan, Evaluation of solar disinfection of E. coli under Sub-Saharan field conditions using a 25L borosilicate glass batch reactor fitted with a compound parabolic collector, Sol. Energy. 100 (2014) 195–202, https://doi.org/10.1016/j.solener.2013.12.011.
[46] K.G. McGuigan, F. Mendez-Hermida, J.A. Castro-Hermida, E. Ares-Mazas, S. C. Kehoe, M. Boyle, C. Sichel, P. Fernandez-Ibanez, B.P. Meyer, S. Ramalingham, E. A. Meyer, F. Méndez-Hermida, J.A. Castro-Hermida, E. Ares-Mazás, S.C. Kehoe, M. Boyle, C. Sichel, P. Fernández-Ibáñez, B.P. Meyer, S. Ramalingham, Batch solar disinfection inactivates oocysts of Cryptosporidium parvum and cysts of Giardia muris in drinking water, J Appl Microbiol. 101 (2006) 453–463, https://doi.org/10.1111/j.1365-2672.2006.02935.x.
[47] H. Gómez-Couso, M. Fontán-Sainz, K.G. McGuigan, E. Ares-Mazás, Effect of the radiation intensity, water turbidity and exposure time on the survival of Cryptosporidium during simulated solar disinfection of drinking water, Acta Trop. 112 (1) (2009) 43–48, https://doi.org/10.1016/j.actatropica.2009.06.004.
[48] J. Ndounla, C. Pulgarin, Solar light (hv) and H2O2/hv photo-disinfection of natural alkaline water (pH 8.6) in a compound parabolic collector at different day periods in Sahelian region, Environ. Sci. Pollut. Res. 22 (21) (2015) 17082–17094, https://doi.org/10.1007/s11356-015-4784-0.